A power pulsed low-pressure argon microwave plasma investigated by Thomson scattering : evidence for molecular assisted recombination

Document Version:
Publisher's PDF, also known as Version of Record (includes final page, issue and volume numbers)

Please check the document version of this publication:

• A submitted manuscript is the version of the article upon submission and before peer-review. There can be important differences between the submitted version and the official published version of record. People interested in the research are advised to contact the author for the final version of the publication, or visit the DOI to the publisher's website.
• The final author version and the galley proof are versions of the publication after peer review.
• The final published version features the final layout of the paper including the volume, issue and page numbers.
Link to publication

Download date: 04. Oct. 2023

A power pulsed low-pressure argon microwave plasma investigated by Thomson scattering:

evidence for molecular assisted recombination

A power pulsed low-pressure argon microwave plasma investigated by Thomson scattering: evidence for molecular assisted recombination

S Hübner, J M Palomares, E A D Carbone and J J A M van der Mullen

Department of Applied Physics, Eindhoven University of Technology, PO Box 513, 5600 MB Eindhoven, The Netherlands

E-mail: S.Huebner@tue.nl and J.J.A.M.v.d.Mullen@tue.nl

Abstract
A squared-wave power pulsed low-pressure plasma is investigated by means of Thomson scattering. By this method the values of the electron density and temperature are obtained, directly. The plasma is created by a surfatron launcher in pure argon at gas pressures of 8–70 mbar. Features of the pulse rise and decay are studied with microsecond time resolution. During the pulse rise we observe initial high temperature values, while the density is still rising. At power switch-off we find decay times of the electron density that are smaller than what is expected on the basis of diffusion losses. This implies that the dominant decay mechanism in the studied pressure regime is provided by molecular assisted recombination.

(Some figures may appear in colour only in the online journal)

1. Introduction

Microwave-induced plasmas (MIPs) are successfully applied in industry for depositing, etching and coating applications [1]. There is a wide variety of MIPs that can be classified as cavities (resonators), surface wave plasmas, torches or micro-plasmas. Surface wave plasmas are characterized by a plasma-creating electromagnetic wave propagating along a plasma–dielectric interface. Examples of surface wave launchers include the surfatron and the surfaguide [2]. An easy way to produce surface wave sustained plasmas at low and intermediate pressure is offered by the surfatron, the launcher dealt with in this study. Its flexibility is one of the reasons why surfatron-induced plasmas are extensively used and studied.

Due to the small sizes and corresponding large gradient strengths, these plasmas are far from equilibrium. So the quasi-steady state is based on a violent competition between plasma creation and destruction mechanisms. For the first category we have to think about ionization processes and for the second on the combination of diffusion and recombination processes. In order to understand the importance of the various processes one can apply relaxation techniques. This can be done by power interruption (PI) or more general power modulation

(PM). The response of the plasmas to PM can be studied using several measurement techniques, for instance using Langmuir probes [3, 4], interferometric methods [5–8], optical emission spectroscopy [9–12] and Thomson scattering (TS) [13, 14]. To come to a better understanding of the temporal response of the plasma and the relation of this response to the corresponding steady-state conditions one should compare experimental results with those of modelling. For examples of model studies of PM we refer to [15–17].

Our experiment is designed to perform TS measurements in power modulated surface wave discharges. In the past this method was applied in our laboratory to study the PI of atmospheric ICPs as performed by De Regt and Van de Sande [13, 14]. To our knowledge, this is first time that this approach has been applied to mw-plasmas. Compared with optical emission spectroscopy, TS has the advantage of giving direct insight into the properties of the electron gas, i.e. the electron density n_e and temperature T_e. The interpretation of the TS results is quite straightforward and does not depend on the plasma state of equilibrium departure. The advantage with respect to probe measurements is that in contrast to probes the laser is, for moderate intensities, not interfering with EM-fields [18]. In contrast to almost all other techniques
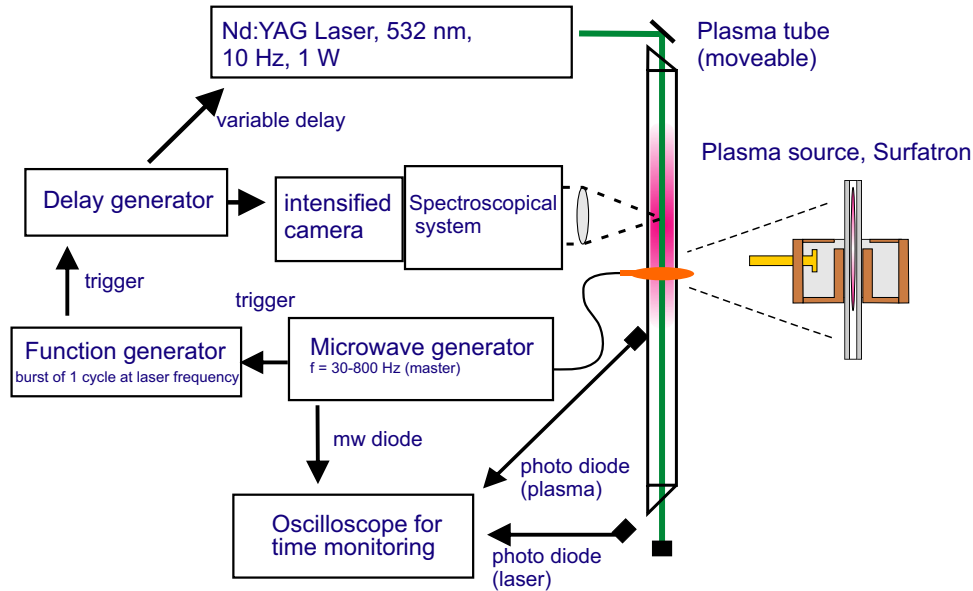
Figure 1. Scheme of the experimental setup. The master signal comes from the microwave generator. To make time-resolved measurements, variable delays can be applied to the laser and the camera. Diodes monitor the mw-pulse, the laser and the plasma light emission.

TS gives excellent spatial resolution. The detection volume formed by the intersection of the laser beam and the line-of-sight of the spectrometer can be rather small; in our study the diameter of that is in the order of 0.1 mm. This is not the case for mw-interferometry and OES where the signal is based on a line-of-sight observation. Moreover, in contrast to most of the other techniques we get an excellent time resolution since the laser pulse has a width in the order of 15 ns. The disadvantage of TS is that the operation of the system, the technique and the procedure are demanding. Moreover, care has to be taken that the laser does not heat the plasma [18]. This can be avoided by tuning the laser power and controlling the focusing.

This paper is organized as follows. In section 2 the experimental setup is described, in section 3 the applied time-resolved TS method is explained and in section 4 the results of the plasma onset and decay are shown and discussed. A concluding section is allocated to a more detailed discussion about the decay mechanism.

2. Experimental setup and TS

Our experiments were performed on a surfatron discharge driven by microwaves with a frequency of 2.45 GHz. This type of device is a well-known plasma source [19, 20]. The surfatron launcher is placed around a cylindrical quartz tube with an inner radius of 3 mm in which the plasma is ignited. We worked with argon in the gas pressure range 8–70 mbar with power pulse frequencies of 30–800 Hz and variable duty cycle. To monitor the power a Schottky-diode is connected to the transmission line between generator and surface wave launcher showing the direct input microwave power. At a typical input power of 67 W the total discharge length is about 51 cm in steady state for a gas pressure of 20 mbar.

For the laser scattering a Nd : YAG 532 nm laser is aligned along the surfatron axis [21]. The photons of the laser beam are scattered on either bound or free electrons, which creates,

respectively, Rayleigh- and Thomson-scattered photons. The Rayleigh scattering along with false stray light created by the scattering of the laser beam on nearby solid surfaces needs to be filtered out, since it is usually much larger and partially overlaps with the TS signal. For this issue we use a triple grating spectrograph (TGS) in which the two first gratings form a notch filter for the spectral range 532 ± 0.2 nm. Only the spectrally broader signal of TS can pass this filter [22]. After the subsequent dispersion by the third grating the photons are collected by an intensified-CCD camera (Andor iStar743). For more details see [21–23].

The number of scattered photons is directly proportional to the number density of scattering events, thus proportional to n_e. On the other hand the Doppler broadening of the scattered photons gives insight into the electron energy distribution, and therefore in the electron temperature T_e. The detection limit of n_e in this setup is about $n_{e,min} = 10^{18}$ m^{-3} depending on the stray light. The results are typically averaged over 10^4 laser shots, which implies averaging over 10^4 plasma pulses.

3. Time-resolved measurements

The timing scheme of the experiment can be seen in figure 1. The master signal for triggering comes from the microwave generator. The minimum pulse length that could be set is 0.2 ms while the highest possible repetition frequency is 800 Hz. Subsequently a function generator is triggered, that works as a pulse-picker corresponding to the 10 Hz operating frequency of the laser. The laser and the iCCD camera are controlled by a delay generator triggered by the mentioned function generator. A variable delay enables time-resolved measurements. In that way the laser is synchronized with the camera and the plasma, even though the plasma could be operated with a much higher power pulse repetition rate. The jitter due to the function generator, the delay generator, the laser and the camera is below 5 ns and negligible compared
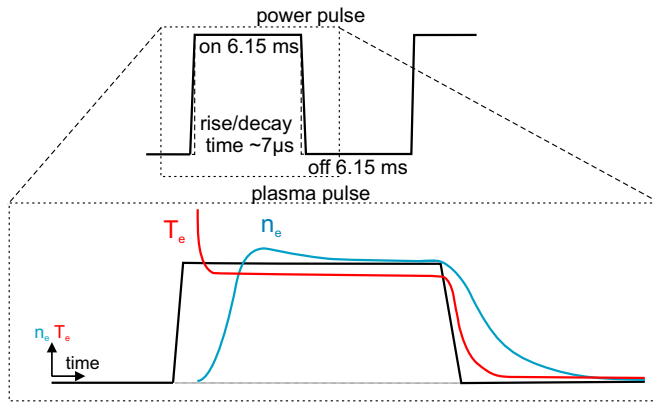
Figure 2. Time scheme of a pulsed microwave plasma at a pulsing frequency of about 81 Hz with a duty cycle of 50%. The modulation depth is 100%, meaning that the power supplied to the plasma between the power pulses is zero. The response of T_e and n_e is shown schematically.

Figure 3. The first 4 ms of the on-period of an 8 (70) mbar Ar plasma pulse powered by 67 W; T_e (right), n_e (left), microwave power in a.u.

with the pulse-to-pulse jitter of the plasma. It was observed that the microwave pulse length has a jitter of about $1\,\mu s\,ms^{-1}$ pulse length. This means that shorter pulses show a better time resolution. We select a repetition rate of 81 Hz with a duty cycle of 50% which implies that the power-on period of 6.15 ms is followed by an off period of 6.15 ms.

4. Results

4.1. Trend of the power pulse

By changing the delay between the power supply and TS system the whole plasma pulse can be scanned. A general trend in terms of n_e and T_e is depicted in figure 2. For the 20 mbar plasma case n_e rises in the beginning of the pulse from a value below $1 \times 10^{18}\,m^{-3}$ (the detection limit of the TS setup) to values around $8 \times 10^{19}\,m^{-3}$. After the initial rising phase n_e drops to around $5 \times 10^{19}\,m^{-3}$ in the end of the pulse, where the plasma reaches a quasi-steady state. After switching off the power, n_e drops exponentially with a certain time constant $\tau_{n_e}^{off}$, which is in the order of $40\,\mu s$. It has to be stressed that the overshoot of n_e observed in the first part of the power-on pulse is about 16% higher than the value in a continuous plasma with the same input power.

The behaviour of T_e in the plasma (re-)ignition is somewhat opposite to that of n_e: the very first measurable data points show very high temperatures, i.e. larger than 3 eV. Subsequently T_e drops to values of 1.0–1.3 eV when approaching a quasi-steady state. When switching off the power T_e follows the power decay very closely. This decay is always faster than that of n_e.

4.2. The plasma onset

This section deals with the ignition phase of the plasma. In figure 3 the first 4 ms of the on-period of the mw-power pulsed plasma is presented for two different pressures. We recall that the power is completely off between the pulses. After the microwave power is switched on, there is a certain time span in which T_e and n_e cannot be measured. This delay, based on
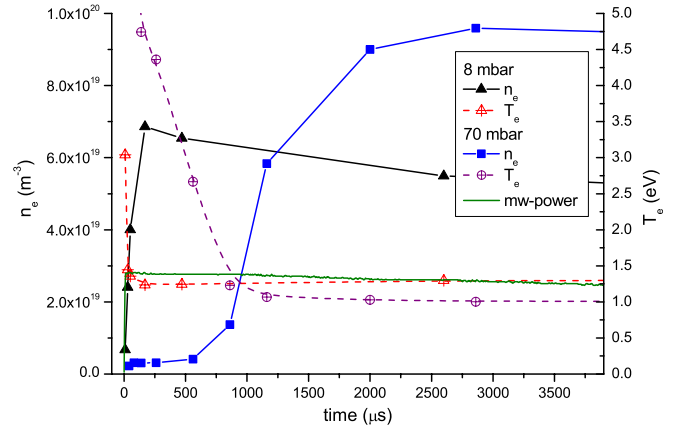
the detection limit of the TS setup, depends on the pressure and ranges from below $5\,\mu s$ for 8 mbar up to $200\,\mu s$ for 70 mbar. Then the values of T_e and n_e take between $180\,\mu s$ (at 8 mbar) up to 2 ms (at 70 mbar) to reach the maximum in n_e and the minimum in T_e.

To explain the T_e behaviour at the pulse onset, the following scenario is proposed. The initial mw-power is transferred to the few first electrons, thus they gain high temperatures. Consequently these electrons ionize the background gas very efficiently. This gives rise to a large population of new electrons that, due to the fact that they are higher in number, get less energy per electron; meaning that the electron temperature is decreased. After that the system approaches a quasi-steady state condition. Hence, the high T_e-values can be understood as a plasma response to the steep mw-power pulse. These results agree with findings by [9, 14], where a high initial T_e value was seen in an atmospheric pressure ICP. Ashida *et al* [3] moreover found that, for a longer power-off duration, the T_e peak is higher. This means that the character of the re-igniting plasma depends on the duration of the power-off period.

As mentioned before there is also an overshoot of n_e in the beginning of the power pulse. At constant duty cycle we observed that the n_e-overshoot for our pressure range is the stronger the lower the pressure is. For high gas pressure (70 mbar) the n_e-overshoot behaviour becomes a more monotone rising of n_e towards the quasi-steady state plasma condition. This is confirmed by the findings in [14] where due to the high pressure of $p = 1$ bar no n_e-overshoot was seen, whereas Ashida *et al* and Behle *et al* [3, 4] reported a similar n_e-overshoot for a low-pressure RF and a microwave slot-antenna discharge, respectively. The overshoot behaviour can be explained by the transient state of the plasma in this early pulse-stage. The initial rise of n_e created by the relatively high T_e values is not yet balanced by the losses effectively. We found experimentally that at 8 mbar a time of $80\,\mu s$ is needed for the effective decay of the steady-state plasma (figure 4). However, the creation time, the time needed to reach the steady-state n_e-density in the power pulse beginning is roughly $50\,\mu s$. This implies a strong overshoot. For higher gas pressure the overall

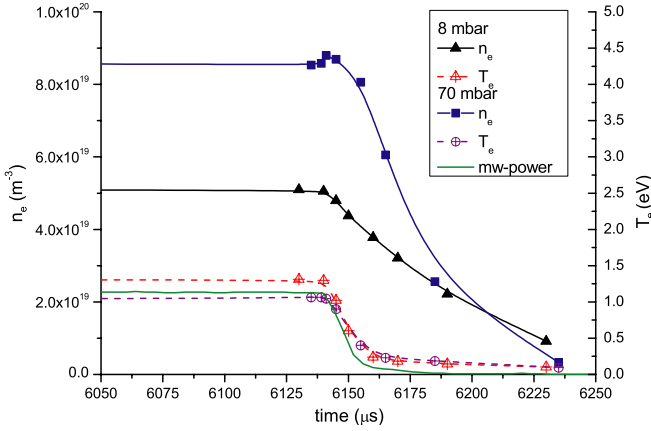J. Phys. D: Appl. Phys. **45** (2012) 055203

S Hübner *et al*

Figure 4. The last part of the power-on and the first part of the power-off phase showing the decay of the electron density and temperature for two pressure cases; same conditions as in figure 3; T_e (right), n_e (left), and microwave power.

Table 1. Pulsed discharge decay parameter.

Ar gas pressure (mbar)	$\tau_{n_e}^{off}$ (μs) for n_e	$\tau_{T_e}^{off}$ (μs) for T_e	T_e(baseline) (K)
8	80 ± 2	7.7	1200
20	42 ± 2	10	1200
40	36 ± 8	6.4	1300
70	30 ± 6	6.8	1250

process of approaching steady state is much slower, so that no overshoot will be present.

4.3. The plasma pulse decay

The decay of the plasma parameters n_e and T_e is shown in more detail in figure 4. The observed decay of the power, i.e. the $1/e$-value, is in the order of $7\,\mu$s; T_e follows this power drop very closely $\tau_{T_e}^{off} \approx 8 \pm 2\,\mu$s. The drop of T_e after power-off is based on the cooling of electrons by elastic and inelastic collisions with argon atoms and ions [13]. This is a much faster process than the decay of n_e which is controlled by diffusion and recombination. Moreover, it is a much faster process than the jitter in time of our system, which is determined by the microwave generator. Thus the T_e drop is indistinguishable from the power drop. The T_e-value drops asymptotically to values around 1200 K. Later in time TS fails to give reliable temperatures since n_e is in the order of the detection limit. We expect that the temperature drops further to the gas temperature.

The n_e decays with a time constant $\tau_{n_e}^{off}$ between 30 and $80\,\mu$s for pressures of 70 to 8 mbar. A summary is given in table 1.

4.4. The decay of the electron density

The study of the temporal evolution of n_e will be guided by the electron particle balance

$$\frac{\partial n_e}{\partial t} = n_e n_a k_{ion} - \frac{D_a n_e}{R^2} - n_e \Omega_{rec} \qquad (1)$$

Table 2. Gas temperatures and molecular ion fractions

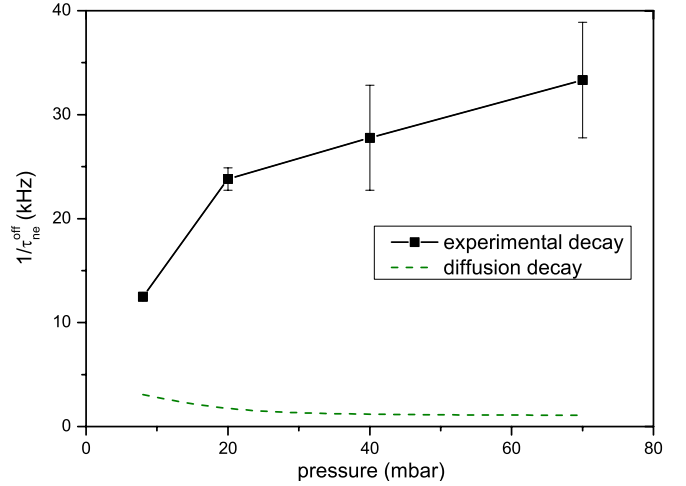| Ar gas pressure (mbar)	T_g (K) from (A.2)	$n_{Ar_2^+}/n_e$ in 10^{-3} from (10)
8	470	0.78
20	590	2.63
40	800	3.09
70	880	10.2

Figure 5. Comparison of the measured decay (full curve) and the calculated diffusion decay (dashed curve) frequency as a function of the gas pressure.

where k_{ion} is the rate coefficient of the effective ionization process, D_a the classical ambipolar diffusion coefficient and R the diffusion length. Assuming a radial Bessel profile of the electron density, the gradient length is $R = a/2.405 \approx 1.2\,$mm. In the last term of this equation, Ω_{rec} represents the effective recombination frequency.

From the results given in figure 4, it can be seen that the decay of T_e is much faster than that of n_e. Thus, we can neglect the ionization processes after power-off and write:

$$\frac{\partial n_e}{\partial t} = -\frac{D_a n_e}{R^2} - n_e \Omega_{rec}. \qquad (2)$$

The decay time of ambipolar diffusion can be estimated and compared with the measured $\tau_{n_e}^{off}$. For the diffusion we used the hard sphere approximation of ion diffusion with a factor for the ambipolar field enhancement [24], i.e. $D_a = 1/(\sqrt{2}n_a\sigma_{a-i})v_{th}(1 + T_e/T_g)$. Where σ_{a-i} is the total neutral-ion cross section and v_{th} the thermal velocity. The employed T_g values are shown in table 2. The calculation of T_g can be found in the appendix. The diffusion decay frequencies $\nu_{diff} = D_a/R^2$ are shown in figure 5 as a function of the gas pressure. Apparently for pressures above 8 mbar the diffusive losses are always much smaller than the observed recombination time of n_e. For that reason we can reduce the particle balance to

$$\frac{\partial n_e}{\partial t} = -n_e \Omega_{rec}. \qquad (3)$$

Now the question emerges what mechanism is responsible for the n_e decay. The $2e^-$ recombination can be evaluated
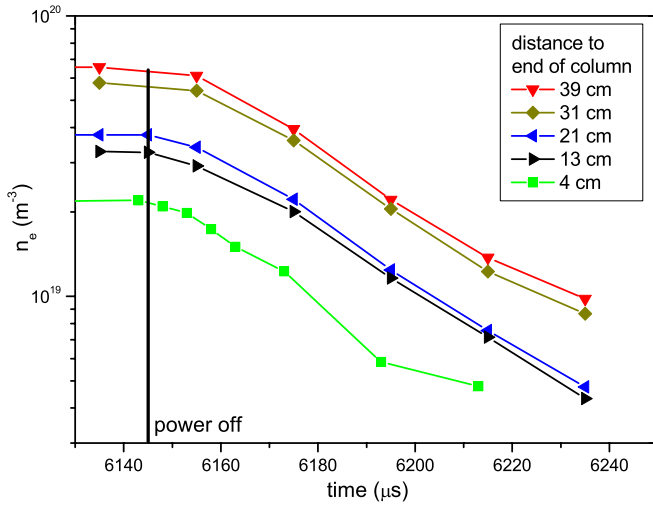
Figure 6. Decay of n_e in the power-off period for different axial positions from the end of the plasma column in a surfatron discharge in argon at 20 mbar.

numerically to be very slow. This is due to the low density of n_e and due to the small rate coefficient because of the relative high T_e-values. Using the well-known Thomson-like formula $\alpha_{2e}^{rec} = 1 \times 10^{-31}(T_e/300)^{-4.5}\,\mathrm{m^{-6}\,s^{-1}}$ [25] we find for $T_e = 0.4\,\mathrm{eV}$, as a typical value of T_e in the decay phase, $\alpha_{2e}^{rec} = 4.3 \times 10^{-37}\,\mathrm{m^{-6}\,s^{-1}}$. This predicts for $n_e = 4 \times 10^{19}$ a decay frequency of 700 Hz. Compared with the measured decay frequencies given in figure 5 this is very small.

Another way to investigate the impact of the $2e^-$ recombination is to measure the plasma pulse decay for different n_e values. In this method we take advantage of the fact that for surfatron plasmas in steady operation, the n_e-value decreases almost linearly as a function of the distance to the launcher [21]. Hence, we simply moved the same discharge and measured the decay at different axial positions. The results for the 20 mbar case are presented in figure 6. To all of these data an exponential fitting was applied to determine a decay constant $\tau_{n_e}^{off}$. The results agree with each other in $\tau_{n_e}^{off} = (42 \pm 2)\,\mu s$. This proves that the decay time does not depend on n_e in the measured range.

But what does that tell us about the explanation for the fast electron decay? The conclusion we can draw is that the decay is driven by recombination and that $\tau_{n_e}^{off}$ does not depend on n_e but on the gas pressure (cf table 1). Based on these findings we must conclude that the decay in this pressure regime is mainly driven by molecular assisted recombination (MAR). This is the recombination due to the formation and subsequent destruction of molecular ions. The formation process is given by the ion-conversion (IC) reaction

$$2\mathrm{Ar} + \mathrm{Ar}^+ \rightarrow \mathrm{Ar}_2^+ + \mathrm{Ar}, \qquad (4a)$$

with rate

$$K_{IC} = 2.5 \times 10^{-43}(300/T_g)\,\mathrm{m^6\,s^{-1}}\ [26], \qquad (4b)$$

while the destruction is given by dissociative recombination (DR)

$$\mathrm{Ar}_2^+ + e^- \rightarrow \mathrm{Ar}^{**} + \mathrm{Ar}^0 \qquad (5a)$$

with rate

$$K_{DR} = 8.5 \times 10^{-13}(T_e/300)^{-0.67}$$
$$\times (T_g/300)^{-0.58}\,\mathrm{m^3\,s^{-1}}\ [15, 27]. \qquad (5b)$$

For estimating the frequency of the processes we take as conditions $p = 20\,\mathrm{mbar}$; $T_g = 590\,\mathrm{K}$; $T_e = 0.4\,\mathrm{eV} = 4700\,\mathrm{K}$ and $n_e = 4 \times 10^{19}\,\mathrm{m^{-3}}$. Inserting these parameter-values in (4b) we obtain

$$\nu_{IC} = n_a^2 K_{IC} = 7.8\,\mathrm{kHz}$$

While (5b) gives

$$\nu_{DR} = n_e K_{DR} = 3600\,\mathrm{kHz}.$$

This means the IC process is much slower and acts as the chain-limiting role in the formation and subsequent destruction of Ar_2^+.

Now, the electron particle balance (equation (2)) can be rewritten including the measured loss frequency ν_{meas} in which the recombination term is replaced by IC. Since $n_e \approx n_{\mathrm{Ar}^+}$ we can write

$$\frac{\partial n_e}{\partial t} = -\frac{D_a n_e}{R^2} - K_{IC} n_a^2 n_e \qquad (6)$$

which leads to

$$\nu_{meas} = \frac{D_a}{R^2} + 1.5 \times 10^{-2}\left(\frac{300}{T_g}\right)^3 p^2 \qquad (7)$$

where p is the gas pressure. Since the lhs is obtained by measurements, we can use this formula to validate the rate coefficient of K_{IC}. To that end we use the data obtained for the 70 mbar case, where diffusion is the slowest. With values of $T_g = 880\,\mathrm{K}$, the measured decay frequency $\nu_{meas} = 33\,\mathrm{kHz}$ and $\nu_{diff} = 1\,\mathrm{kHz}$ from figure 5 we obtain

$$\frac{\nu_{meas} - \nu_{diff}}{n_a^2 K_{IC}} = 0.6. \qquad (8)$$

This is a fair agreement, taking into account that no other rates are considered and that the error bars on the measured decay constant are about 17%. The measurements for all pressure together give a ratio of 1.6 ± 1. This agreement of the IC rate proves that the decay is indeed chain-limited by IC.

The strong dependence of the decay time on the gas temperature suggests also using the opposite approach: use the decay measurements as thermometer. In the high pressure regime (>8 mbar) when IC is far dominant over diffusion, the decay of n_e after the plasma pulse directly correlates with p^2/T_g^3 which can be used for determining T_g values.

But what is the next step in the recombination process? The Ar_2^+ molecules recombine very fast to ground state or excited state argon atoms. Based on the DR-rate (4) and IC-rate (5) we can calculate an approximate Ar_2^+ ion fraction ratio in a two-rate balance

$$\frac{n_{\mathrm{Ar}_2^+}}{n_{\mathrm{Ar}^+}} = \frac{\nu_{IC}}{\nu_{DR}} \qquad (9)$$

which, on employing (4b) and (5b) gives the expression

$$\frac{n_{\mathrm{Ar}_2^+}}{n_{\mathrm{Ar}^+}} = 1.71 \times 10^{10}(300/T_e)^{-0.67}(300/T_g)^{2.42}p^2 n_e^{-1}. \quad (10)$$

Inserting for $T_e = 0.4$ eV, n_e and the estimations for T_g give values of $n_{Ar_2^+}/n_{Ar^+} = 8 \times 10^{-4}$ (10×10^{-3}) for pressures of 8 (70) mbar presented in table 2. The diffusion is not taken into account here, but that introduces only minor changes in the results. The small fraction of molecular ions should not disguise the importance of the MAR-channel in the recombination of ions. It is rather an illustration of the high DR rate.

The uncertainties in the rate coefficients, the gas temperature and the reproducibility of the plasma determine the error of $n_{Ar_2^+}/n_e$. This leads altogether to an error of 40%, which seems large but comparison with model results shows that the error bar is not large enough to cover the wide spread of values predicted by models such as [15, 28].

There are remaining issues that have to be addressed in future studies. One of the topics is whether the MAR is (partially) balanced by re-ionization of its products, the excited argon atoms. Another issue is the local dependence of the presented results.

5. Summary

A power-interrupted surface-wave-induced plasma was investigated by means of Thomson scattering. With this method we could obtain the precise local response of the n_e and T_e-values to the power pulse.

High T_e-values are seen in the beginning of the power pulse followed by T_e approaching a steady-state value. After switching off the power, T_e decays fast with a decay time comparable to that of the microwave power supply.

Upon switching on the power, we observe an initial rise in n_e reaching an overshoot with respect to the steady-state value. This overshoot is higher for lower gas pressures. The decay of n_e after the pulse termination is slower than for T_e and in the order of 30–80 μs.

Evaluating the electron particle balance shows that diffusion is not sufficient to explain the relatively fast decay of n_e so that we have to conclude that MAR is the predominant electron loss mechanism in surfatron plasmas with argon pressures above 10 mbar. The chain-limiting process is the three-body ion conversion $Ar^+ \rightarrow Ar_2^+$. Based on the rate balance of formation and destruction of Ar_2^+ we found molecular ion fractions $n_{Ar_2^+}/n_{Ar^+}$ that are in the range 0.3% (1%) for 20 (70) mbar.

Acknowledgments

Appendix. The gas heating in a surfatron plasma

In [29] it was found that the gas temperature in a surfatron argon-plasma can be approximated quite well using Fourier's law. The dominant heating is performed by elastic electron–atom collisions, so we can write the energy balance as

$$n_a n_e K_{heat} k_B (T_e - T_g) = -\frac{\lambda_H}{R^2}(T_g - T_{wall}) \qquad (A.1)$$

where K_{heat} is the electron–argon heat transfer rate, λ_H the thermal conductivity and $T_{wall} \approx 450$ K is the wall temperature. For R, the gas temperature gradient length, we take the n_e-gradient length. Using $T_e \gg T_g$ this expression becomes a quadratic equation for T_g with the solution

$$T_g = \frac{T_{wall}}{2}(1 + (1 + 4C(pn_e k_B T_e)/T_{wall}^2)^{1/2}) \qquad (A.2)$$

where $C = K_{heat}(k_B \lambda_H)^{-1} R^2$. This equation was used to calculate T_g using experimentally determined values of n_e, T_e and p. The values $\lambda_H = 0.0178$ W $(m^{-1} K^{-1})$ and $K_{heat} = 6.7 \times 10^{19}$ m^3 s^{-1} are taken from the literature [29]. The results for different pressures can be found in table 2.

References

[1] Moisan M and Pelletier J 1992 *Microwave Excited Plasmas, Plasma Technology* vol 4 (The Netherlands: Elsevier Science Publishing)
[2] Moisan M and Zakrzewski Z 1991 *J. Phys. D: Appl. Phys.* **24** 1025–48
[3] Ashida S, Shim M R and Lieberman M A 1996 *J. Vac. Sci. Technol.* A **14** 391
[4] Behle St, Brockhaus A and Engemann J 2000 *Plasma Sources Sci. Technol.* **9** 57–67
[5] Cotrino J, Gamero A, Sola A and Colomer V 1988 *J. Phys. D: Appl. Phys.* **21** 1377–83
[6] Armour D G 1974 *J. Phys. B: At. Mol. Phys.* **7** 1213
[7] Berndt J, Kovačević E, Selenin V, Stefanović I and Winter J 2006 *Plasma Sources Sci. Technol.* **15** 18–22
[8] Krämer M, Clarenbach B and Kaiser W 2006 *Plasma Sources Sci. Technol.* **15** 332–7
[9] Fey F H A G, Stoffels W W, van der Mullen J A M, van der Sijde B and Schram D C 1991 *Spectrochim. Acta* B **46** 885–900
[10] Bydder E L and Miller G P 1988 *Spectrochim. Acta* B **43** 819–29
[11] Kafrouni H, Bagneux J M, Gleizes A and Vacquie S 1979 *J. Quant. Spectrosc. Radiat. Transfer* **21** 457–73
[12] Garcia M C, Rodero A, Sola A and Gamero A 2000 *Spectrochim. Acta* B **55** 1611–21
[13] de Regt J M, van der Mullen J J A M and Schram D C 1995 *Phys. Rev.* E **52** 2982–87
[14] van de Sande M J, van Eck P, Sola A, Gamero A and van der Mullen J J A M 2003 *Spectrochim. Acta* B **58** 783–95
[15] Bogaerts A 2007 *J. Anal. At. Spectrom.* **22** 502–12
[16] Lieberman M A and Ashida S 1996 *Plasma Sources Sci. Technol.* **5** 145–58
[17] Fey F H A G, Benoy D A, van Dongen M E H and van der Mullen J A M 1995 *Spectrochim. Acta* B **50** 51–62
[18] Carbone E A D, Palomares J M, Hübner S, Iordanova E and van der Mullen J J A M 2012 *J. Instrum.* **7** C01016
[19] Moisan M, Zakrzewski Z and Pantel R 1979 *J. Phys. D: Appl. Phys.* **12** 219–37
[20] Zhelyazkov I and Atanassov V 1995 *Phys. Rep.* **255** 79–201
[21] Palomares J M, Iordanova E, van Veldhuizen E M, Baede L, Gamero A, Sola A and van der Mullen J J A M 2010 *Spectrochim. Acta* B **65** 225–33
[22] van de Sande M J, Deckers R H M, Lepkojus F, Buscher W and van der Mullen J J A M 2002 *Plasma Sources Sci. Technol.* **11** 466–75

[23] van de Sande M J and van der Mullen J J A M 2002 *J. Phys. D: Appl. Phys.* **35** 1381–91

[24] Mitchner M and Kruger C H 1973 *Partially Ionized Gases* (New York: Wiley)

[25] Biondi M A 1982 *Applied Atomic Collision Physics* vol 3 *Gas Lasers* (New York: Academic) chapter 6

[26] Hawley M and Smith M A 1992 *J. Chem. Phys.* **96** 326

[27] Mehr F J and Biondi M A 1968 *Phys. Rev.* **176** 322–6

[28] Jonkers J, van de Sande M J, Sola A, Gamero A, Rodero A and van der Mullen J J A M 2003 *Plasma Sources Sci. Technol.* **12** 464–74

[29] Iordanova E 2010 Polydiagnostic validation of spectroscopic methods *PhD Thesis* Eindhoven University of Technology